Comparison of Experimental and Numerically Obtained Flow Properties of a Bluff Body

Gandert M.R. van Raemdonck, Peter van Leeuwen and Michel J.L. van Tooren

Abstract The expected road transport demand in the next twenty years and the increasing environmental constraints together with the rising fuel prices has renewed the interest in truck design; any reduction in truck fuel consumption can be associated with large annual fuel cost reduction and considerable emission savings. Within the development of aerodynamic solutions numerical analysis tools, based on RANS equations, are often used to indicate flow phenomena and characteristics to design low drag bluff bodies. The presented work will discuss the similarities, but mainly the differences between wind tunnel experiments and the time-averaged numerical analysis. Rear pressure distributions are completely different when the numerical outcome is compared with the wind tunnel experiments. The CFD analysis of the boundary layer thickness is within acceptable resemblance with the wind tunnel measurements and the analytical power law model results. Stereoscopic PIV results show different wake structures.

1 Introduction

The expected road transport demand in the next twenty years and the increasing environmental constraints together with the rising fuel prices has renewed the interest in aerodynamic truck and trailer design in the last decade; any reduction in truck fuel consumption can be associated with large annual fuel cost reductions and considerable emission savings for the transport sector. The environmental concerns and the

G.M.R. van Raemdonck (✉) · M.J.L. van Tooren
Faculty of Aerospace Engineering (TU Delft), Kluyverweg 1, 2629 HS Delft, The Netherlands
e-mail: g.m.r.vanraemdonck@tudelft.nl

M.J.L. van Tooren
e-mail: m.j.l.vantooren@tudelft.nl

P. van Leeuwen
Faculty of Mechanical, Martime and Materials Engineering (TU Delft), Mekelweg 2,
2628 CD Delft, The Netherlands
e-mail: p.m.vanleeuwen@tudelft.nl

harsh competition force the transport companies to reduce fuel consumption in an economically and environmentally sustainable way.

Generally there are two ways to reduce the fuel consumption of a vehicle. One can improve the efficiency of the engine delivering power: improvements on the side of the available power. Or one can lower the different forces acting on a truck travelling over the road: the required power side. The latter can be achieved by reducing the weight of the vehicle, reducing its aerodynamic drag and by reducing the friction resistance of the tires.

Improving the fuel economy of trucks by aerodynamic means has become an accepted practice in the last decades. Truck manufacturers improved the aerodynamic performance of their tractor by applying roof deflectors, side fenders and corner vanes. Many aerodynamic solutions have been developed for the front and top of the tractor and for the gap between the tractor and trailer, [1, 6, 19].

Within the development of these aerodynamic solutions numerical simulations, based on steady Reynolds Average Navier-Stokes equations (RANS), are often used to indicate flow phenomena and characteristics. In order design low drag bluff bodies more insight in the flow behaviour is required as well as in the prediction capability of the used numerical tools.

In 2005 a research program was initiated at the faculty of Aerospace Engineering to reduce the fuel consumption of heavy duty vehicles by lowering the aerodynamic drag of articulated trucks. These types of vehicle are mostly used for long-haul road transport and have a high aerodynamic drag contribution due the bluff shape of the trailer and its high average travelling velocity. The presented research discusses the flow characteristics of a standard model, called Generic European Transport System, by comparing numerical simulations and wind tunnel experiments. The obtained (dis)similarities of several design examples will be discussed.

2 Set-Up

2.1 Truck Model: Generic European Transport System

A new wind tunnel model, in analogy with the GTS model analysed by Gutierrez [7] and Storms [15], is designed that meets the different requirements in order to perform the desired research. This new generic model is based on a European tractor semi-trailer combination used for international road transport and is referred to as GETS, Generic European Transport System, see Fig. 1. The guide lines of the Society of Automotive Engineers concerning wind tunnel testing of bluff bodies SAE J1252 [14] are considered with respect to Reynolds number and blockage effects. The dimensions of the new model are defined and displayed in Fig. 2

The Reynolds number for a European full-scaled truck, based on the square root of the frontal area of $A = 10.34$ m^2, a driving velocity of 25 m/s, air density of 1.225 kg/m^3 and an air viscosity of 1.7894×10^{-5} kg/ms, becomes 5.5×10^6. The
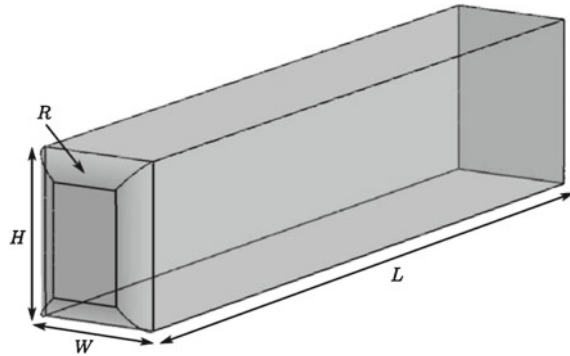
Fig. 1 Generic European transport system model

Fig. 2 Wind tunnel model dimensions

| length L [mm]	1100
width W [mm]	173
height H [mm]	234
ground clearance [mm]	33
front radius R [mm]	36
scale	1:15
ratio frontal area model-section	0.02
ratio width model-section	0.22
ratio height model-section	0.24
test velocity V_t [m/s]	60
Reynolds number, $\sqrt{A}$	0.8264×10^6

Reynolds number in the wind tunnel, with a testing velocity of 60 m/s is 0.8264×10^6 and meets the requirements set by SAE J1252 [14] for bluff bodies.

Front edge separation is undesirable within this research, therefor several radius ratios based on the width of the body and the frontal radius are recommended. Within the experiments of Cooper [3] and Henneman [8] a study is executed on front edge separation of bluff bodies within a certain range of radius ratios. Their experiments showed that a certain transcritical Reynolds number $(Re_r)_t$ based on the radius of the front edge has a constant value of 1.24×10^5 for the turbulence intensity present in the used wind tunnel test section. This transcritical Reynolds number can be defined as

$$(Re_r)_t = \frac{\rho r V_t}{\mu} \tag{1}$$

where ρ is the air density, μ the air viscosity, V_t the test velocity and r resembles the radius of the front edge. In order to calculate the radius of the frontal edges with the above Eq. 1, V_t is set on 50 m/s to increase the velocity range where the boundary layer stays attached. This gives a radius of 36 mm for all the frontal edges.

With a microphone is indicated that an attached and turbulent boundary layer is present at side of the model. Oil visualization identified a small separation bubble just behind the front radius. The separation bubble disappeared after adding zig-zag tape (0.65 mm thickness) in front of the curvature, van Raemdonck [20].

Fig. 3 Reynolds effects
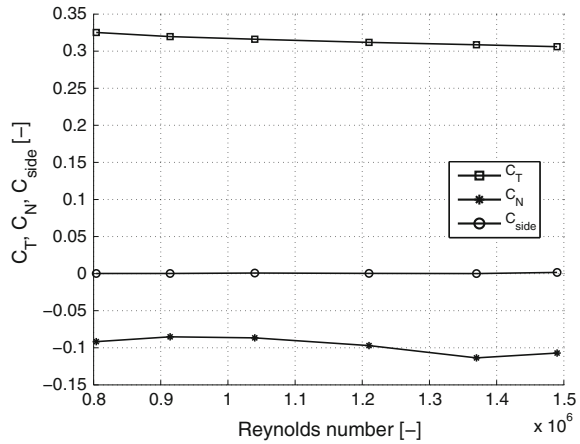
The GETS model is tested within a velocity range of 50–100 m/s in order to detect possible Reynolds effects. As Fig. 3 illustrates no large Reynolds effects are detected within the velocity range.

2.2 Evaluation of Numerical Tools

A surface model of the GETS model is generated based on the dimensions summarized in Fig. 2. Discretization of the volume around the model is done by introducing blocks. A structured surface mesh is extruded normally to create a structured boundary layer mesh. The rest of the volume around the model (length = 25 width, half width = 8 width; height = 11 width) is filled with tetrahedrals. A half model, except for the yaw angle variation, is used for the simulations in order to reduce the amount of cells (total number of cells: 6 million) and the corresponding processing time (Fig. 4).

Fig. 4 CFD surface model together with volume mesh
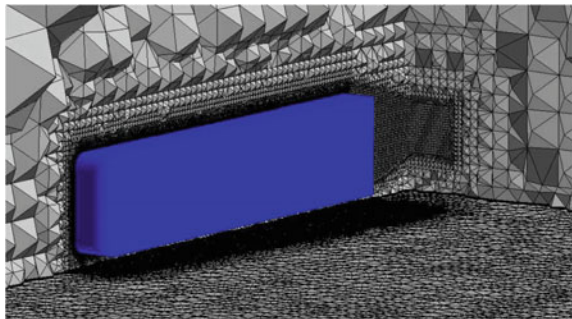
The Reynolds Averaged Navier-Stokes flow equations together with the Realizable $\kappa - \varepsilon$ turbulence model are solved with the commercial package Fluent. There is opted for this type of turbulence model due to the its common usage in the automobile sector, its performance with bluff bodies and its relatively low required computer power, Lanfrit [10]. As near-wall treatment for the boundary layer, the non-equilibrium wall function, is chosen ($30 < y^+ < 300$). The operating pressure of 101325 Pa is defined in one of the outer corners of the computational domain.

The upstream inlet has the velocity inlet boundary condition: an absolute magnitude of 60 m/s in the direction of the flow for 1:15 scaled set-up; 25 m/s for the full-scale situation. The outlet is set as pressure outlet. The actual symmetry plane as well as the other two outer planes (side and upper plane) have the symmetry boundary condition. The floor is defined as a moving wall with a translational velocity as well as a fixed wall or symmetrical plane boundary conditions are simulated.

2.3 Experimental Modeling

The wind tunnel experiments are executed in the atmospheric Low Turbulence Tunnel. This closed circuit wind tunnel has an octagonal test section with a cross sectional area of 2.07 m^2 (width of 1.8 m; height of 1.25 m, Fig. 5) and with parallel wind tunnel walls. The maximum operating velocity of the wind tunnel is 120 m/s; the turbulence intensity can be changed in the range 0.02–0.1 %. The empty test section is calibrated for the wind velocity with the aid of a pitot tube by measuring the dynamic pressure in the centre of the test section and compare it with a static pressure difference between two locations in front of the test section.

The wind tunnel used is not equipped with a moving belt. According to Cooper [4, 5] one can conclude that a fixed-floor with a thinned boundary layer is sufficient for current automotive and commercial vehicle applications. The vehicle model is suspended on a parallel ground board which has an offset of 300 mm with respect to the upper wind tunnel wall and has the same width as the test section, Fig. 5. On the rounded front edge of this ground board develops a new thinner boundary layer.

Fig. 5 Cross section low turbulence tunnel
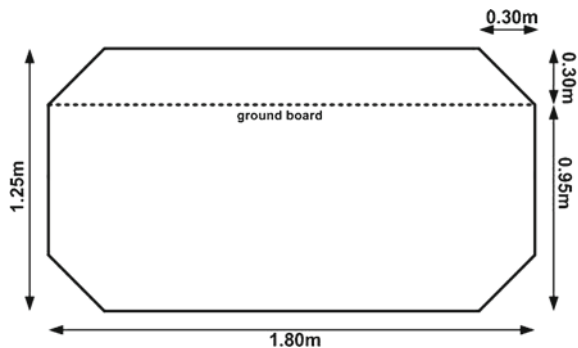
3 Flow Properties of the GETS Model

In this section several flow properties will be analysed and discussed. A comparison will be made between the results of the numerical and the wind tunnel analysis, both for 1: 15 scaled model with a velocity of 60 m/s.

3.1 Force and Pressure Coefficient

An overview of the drag and lift coefficient numerically simulated with different mesh and cell types is given in Table 1. The listed simulations are performed by different students involved in this research project. The difference in the outcome for the coefficients illustrate one has to be careful comparing the absolute drag values.

The bottom half of Table 1 illustrates the corrected (for blockage effects in closed test section) and uncorrected force and pressure coefficient obtained with wind tunnel experiments. A corrected drag and lift coefficient of respectively 0.297 and -0.036 is observed, while a mean rear pressure coefficient of -0.163 is measured.

Comparing the numerical simulations and wind tunnel experiments one can state that the drag and the mean rear pressure coefficients are rather in line which each other, except for the hexahedron mesh. Also a large difference between the simulated and measured lift coefficient can be observed. This is probably due to the fact the wind tunnel is not equipped with a rolling belt to simulate a moving road.

Table 1 Numerical and wind tunnel results: force and pressure coefficients

Numercial results					
Grid type	Scale	Velocity (m/s)	C_D	C_L	$C_{P,base\ mean}$
Tetrahedron [13]	1:15	60	0.3017	-0.1348	-0.1048
Tetrahedron [18]	1:15	60	0.277	-0.136	-0.145
Tetrahedron [18]	1:1	25	0.318	-0.100	-0.133
Polyhedron [13]	1:15	60	0.3023	-0.1412	-0.1194
Hexahedron [17]	1:15	60	0.2399	-0.1635	-0.1483
Wind tunnel results					
	Scale	Velocity (m/s)	C_D	C_L	$C_{P,base\ mean}$
Uncorrected	1:15	60	0.327	-0.080	-0.145
Corrected	1:15	60	0.297	-0.036	-0.163

The numerical simulations resulted in a typical drag breakdown of the GETS model as for a bluff body: 18 % friction drag and 82 % pressure drag, van Leeuwen [18]. The frontal surface, which includes the rounded edges, contributes 41 % which is almost as much as the rear surface: 42 %. The center body only experience friction drag and accounts for 17 % of the total drag of the vehicle.

3.2 Boundary Conditions

With the aid of CFD different boundary conditions for the full-scale GETS model are simulated. Only small relative differences are obtained when a moving ($C_D = 0.318$) or symmetric floor ($C_D = 0.320$) are compared with a stationary wall boundary condition ($C_D = 0.320$). The difference in lift coefficient are larger: $-0.101, -0.093$ and -0.099 for a moving, stationary and symmetric floor respectively.

Figure 6 illustrate how the velocity profile changes near the floor with different boundary conditions for different downstream locations in the near wake. In case of a symmetric floor no boundary layer is formed, while the boundary layers for the moving and stationary floors differ significantly. The velocity in the wake area is below freestream velocity therefor the flow is accelerated by the floor in the moving wall situation opposed to decelerated in the stationary wall simulation.

Although the wake velocity profiles show good agreement between the moving and symmetric wall conditions, except near the ground, the drag coefficient of the symmetric wall is closer to the fix wall simulation. This is remarkable as the velocity profiles of the fixed and the symmetric wall differ more than expected from the difference in C_D value. For the moving wall simulation the suction peak on the lower curved front face is higher compared to the symmetrical case. This suction peak can be explained by the effect that a boundary layer develops on the wall under the model creating a displacement thickness which accelerates the flow passing through the floor and the model, leading to a higher suction peak.
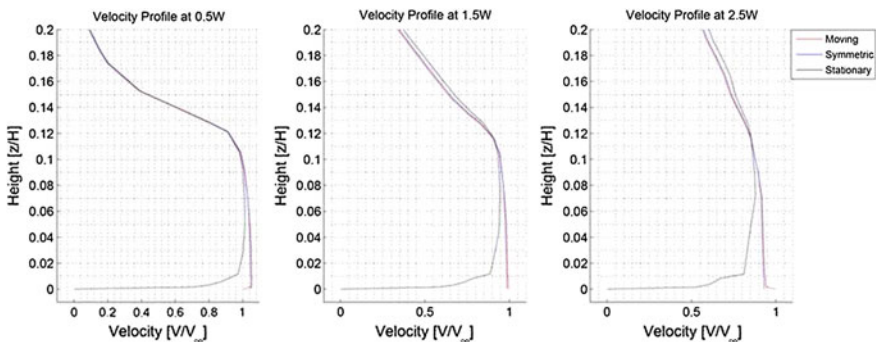

Fig. 6 Rear velocity profiles for different boundary conditions

3.3 Cross Wind Influence

In real case situations a truck is always experiencing cross winds. Cross winds can have a large influence on the total drag C_T and side force C_S due to flow separation on the front-end of the truck.

The force and the mean base pressure coefficients are shown in Figs. 7 and 8 for a certain yaw angle range. The drag coefficient first increases, but remains approximately constant after 6° while the side force coefficient increases. The increased suction peak on the leeward front edge curvature creates a larger forward suction as well as a side ward suction force. The CFD and wind tunnel results follow the same trend, however, the uncorrected data is offset compared to the numerical drag coefficient.

In Fig. 8 the mean base pressure coefficient is illustrated, which decreases with increasing yaw angle, increasing the suction force on the back of the model. With increasing yaw angle the difference between the numerical simulations and the wind tunnel experiments seems to become larger.

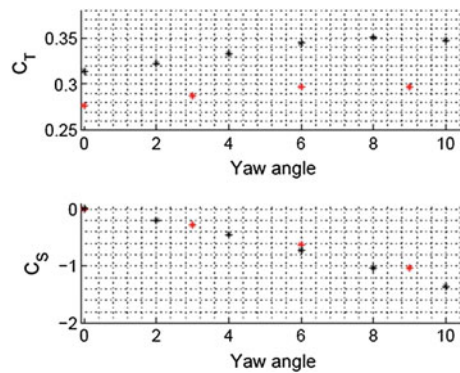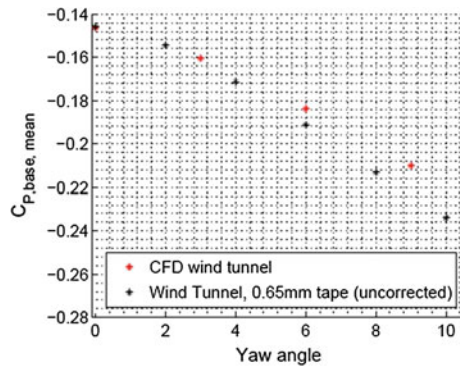**Fig. 7** Drag and side forces in relation with increasing yaw angle

Fig. 8 Rear pressure coefficient in relation with increasing yaw angle

3.4 Boundary Layer Properties

The boundary layer properties on the side surface 15 mm ahead of the rear edge is measured (van Raemdonck, [20]) and compared to simulated values (van Leeuwen, [18]) in Figs. 9 and 10. The latter illustrates different velocity profiles indicating the shape of the simulated, measured and theoretical boundary layers.

The wind tunnel measured values of δ, δ^*, θ and H are in close agreement with the theoretical turbulent flat plate equations. The simulated boundary layer on the scaled model is thicker ($\delta/W = 147$) compared to the flat plate estimation ($\delta/W = 110$) and the wind tunnel measured value ($\delta/W = 105$). Also the displacement thickness and momentum thickness are higher compared to the measured and estimated values. The shape factor H is higher in case of the simulated results, however, it must be noted that, as can be seen in the Fig. 10, there is an irregularity in the simulated results for the wind tunnel boundary layer. This irregularity is due to the interface of the hybrid mesh and the interpolation during the data export.

Compared to the 1/15th scale simulation the full-scale simulation has much fuller profile, also indicated by the lower shape factor H. The difference can be explained by

Fig. 9 Wind tunnel model dimensions

	δ/W $(1e^{-3})$	C_f $(1e^{-3})$	δ^*/W $(1e^{-3})$	θ/W $(1e^{-3})$	H
CFD (1:1)	94	1.62	6.6	5.9	1.13
CFD (1:15)	147	2.51	15.6	11.6	1.34
Wind tunnel	105	-	14	10.4	1.3
Flat plate	110	2.70	13.6	10.7	1.278

Fig. 10 Boundary layer profiles

CFD 1/15th scale
Wind Tunnel, 0.65mm zigzag tape
CFD full scale
1/7th power law (corrected)
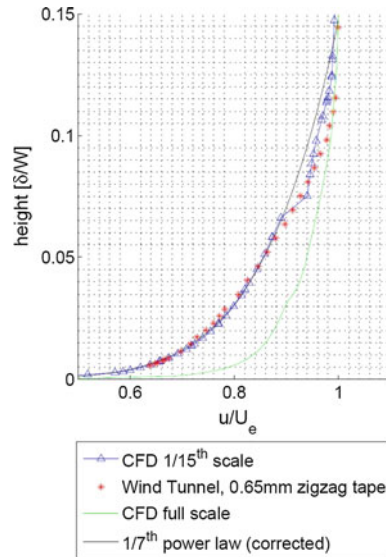
the low freestream turbulence intensity of the wind tunnel compared to the full scale simulations. Numerical diffusion leads to thicker boundary layers at high Reynolds numbers.

3.5 Wake Structure and Streamlines

Figures 11 and 12 illustrate the wake structure obtained with the aid of stereoscopic PIV (Particle Image Velocimetry) and CFD simulation respectively, van Dijk [16]. Both figures show the horizontal velocity magnitude and a projection of the path lines. In general one can observer the two counter rotating vortices inducing a negative static pressure in the near wake of the GETS model.

When one compares both wake structures more closely one can observe that the numerical simulation underestimates the thickness of the boundary layers of the model, especially at lower side and the ground plate. This may result in an overestimation of the size of the lower vortex and underestimation of the upper

Fig. 11 PIV result of the symmetry plane of the wake
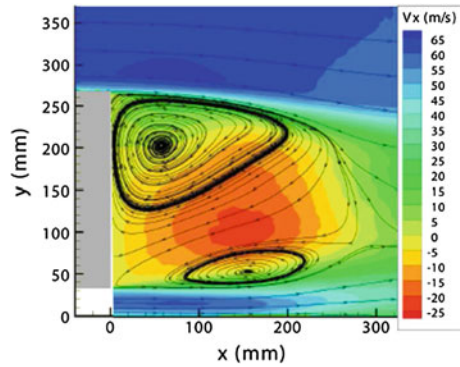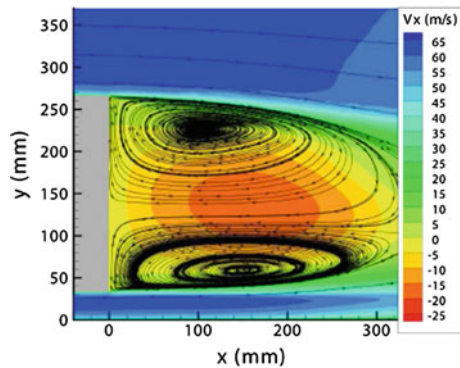
Fig. 12 CFD result of the symmetry plane of the wake

vortex. Clearly visible is that the lower vortex measured in the wind tunnel, see Fig. 11, is smaller than the lower vortex obtained with CFD.

The vertical asymmetry of the two counter rotating vortices is resulting in upstream flow paths that are angle downwards, in stead of horizontally oriented in the numerical simulations. Also the length of the near wake obtained with PIV measurement is much smaller compared with the near wake length resulting from the CFD analysis.

3.6 Rear Pressure Distribution

The rear pressure distribution of the GETS model, obtained with the aid of wind tunnel experiments and numerical simulations are shown in Fig. 13. As can be seen in the contour plots the pressure distribution measured in the wind tunnel differs significantly compared to the simulated distribution obtained with the aid of CFD. There is no pressure maximum close to the center of the base for the wind tunnel results: a more lateral pressure distribution is obtained. Also the minima and maxima of the measured values are completely different compared to the CFD values.

In the case of 6° yaw, see Fig. 14, the flow remains attached on the front of the GETS model, whereas it separates in the wind tunnel data, causing a more asymmetric pressure distribution in the wind tunnel data compared to the CFD results.
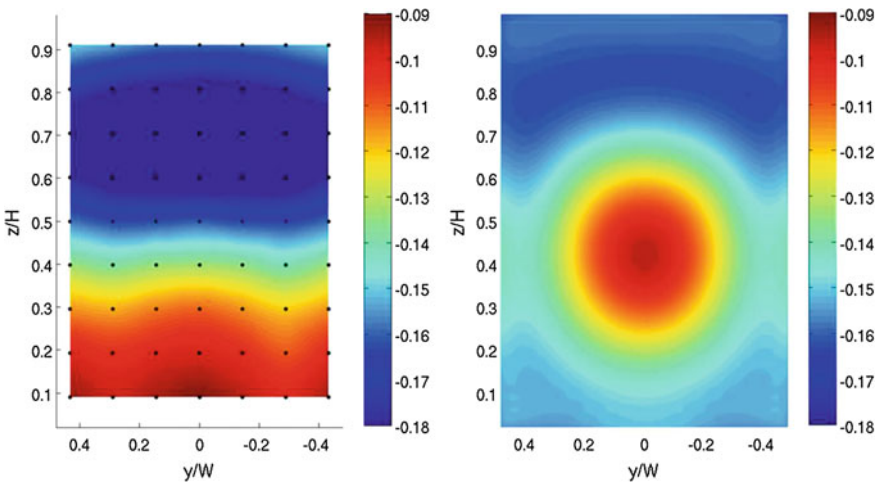

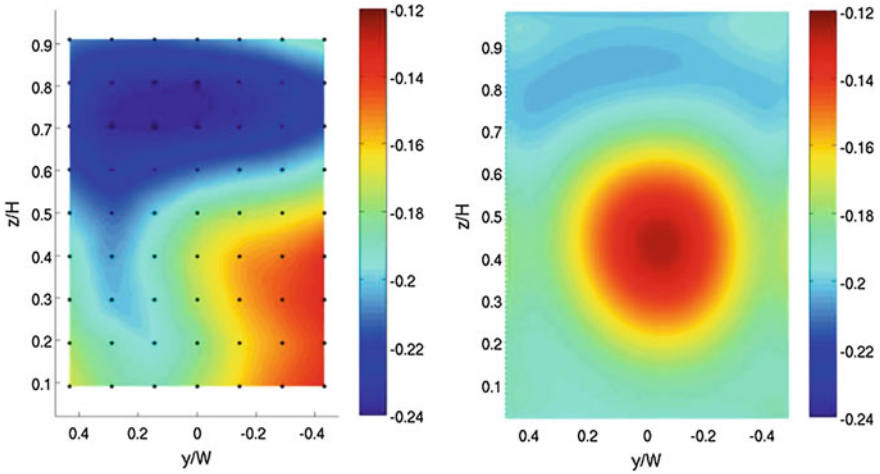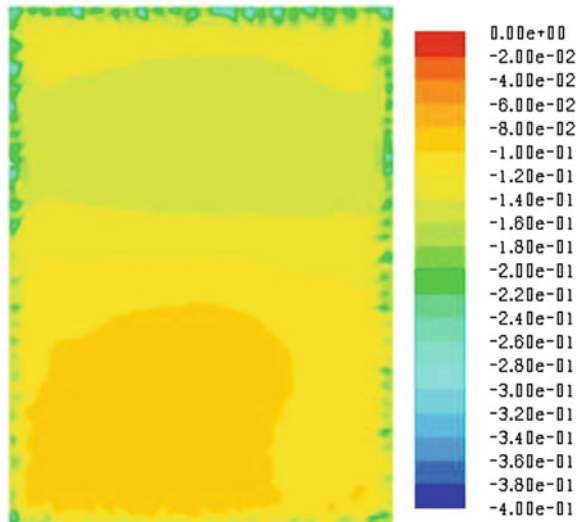**Fig. 13** Rear pressure distribution: (l) wind tunnel experiments and (r) CFD simulation

Fig. 14 Rear pressure distribution at 6 yaw angle: (l) wind tunnel test and (r) CFD simulation

3.7 Turbulence Modeling

In the above comparison analysis steady RANS equations are solved with the aid of the realizable $\kappa - \varepsilon$ turbulence model. Two other turbulence models, SST $\kappa - \omega$ and Reynolds Stress Model (RSM), are applied (Schrijvers [13]) to analyse if an improvement in the prediction of rear pressure distribution and wake structure could be achieved. As expected the obtainded pressure distribution with the two other

Fig. 15 Rear pressure distribution obtained with LES

turbulence models did not match the rear pressure distribution obtained with wind tunnel experiments.

With the RANS mesh a first attempt is undertaken to conduct a Large Eddy Simulation (LES). The velocity is set on 6 m/s and a time step of 1×10^{-4} s is defined. The time-averaged pressure distribution can be observed in Fig. 15. Although the applied mesh was too coarse for this simulation and a velocity of 6 m/s is set, one can see that the LES rear pressure distribution is more similar to the wind tunnel measurements. Identatical observations are made by Krajnović [9].

4 Design Examples

Different flow properties of the GETS model obtained with numerical simulations and wind tunnel experiments are discussed and compared. In the next part different design examples, to obtain a low drag heavy duty vehicle, will be analysed. Typical flow characteristics like pressure distribution and drag coefficient will be analysed. Numerical simulations (based on RANS) will be compared with wind tunnel tests. Both set-ups are executed with 1:15 scaled models and an inlet velocity of 60 m/s.

4.1 Standard and Stepped Boat Tails

Boat tails are a well known concept to reduce the drag of heavy duty vehicles. In this research project different boat tail configurations (i.e. slant angle, offset distance and tail lenght variations) are tested in the wind tunnel and simulated by Vonk [21].

The standard boat tail with flush side panels showed a drag reduction of 39 % during the wind tunnel experiments and in the numerical simulations for the GETS model. Figure 16a, b display the difference in flow between the wind tunnel results and that of the simulations for the standard boat tail. It can be noted that the location of the upper vortex is comparable as is the main direction of the flow. Although the CFD prospects a flow which is more horizontally directed, where the flow of the PIV analysis shows a flow directed towards the upper inner part of the boat tail. Due to the shadow of the upper boat tail element the PIV results do not show the second vortex which should be, conform the numerical simulations, located inside the cavity. Again at the lower side one can observe lower velocities in the wind tunnel experiments induces a different flow field.

The best performing stepped boat tail only indicated a drag reduction of 10 %, Vonk [21]. Figure 16c and d illustrate the velocity field together with the streamlines for a stepped boat tail configuration. Due to the shadow of the stepped tail, the lower small vortex is not visible. The upper vortex structure is clearly visible in the PIV experiments while the CFD simulaitons has difficulties to indicate the structure. The two counter rotating structures in the near wake of the stepped boat tail are clearly present, both in the PIV results and the numerical simulations. The closure of the
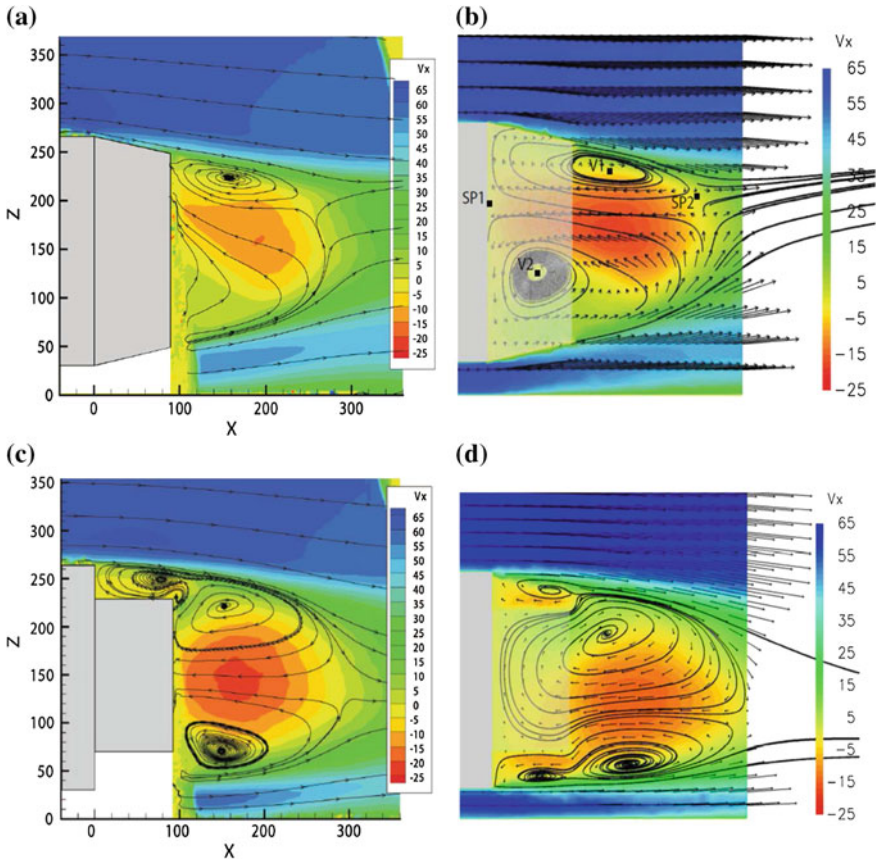
Fig. 16 Streamlines of standard and stepped boat tail on the GETS model **a** PIV result of a standard boat tail. **b** CFD result of a standard boat tail. **c** PIV resuls of a stepped boat tail. **d** CFD result of a stepped boat tal

near wake of the PIV measurement seems to be shorter compared with the numerical simulations. Figure 16c indicates the existance of extra vortex at the rear edge of the stepped boat tail which is not captured with the numerical simulations. This extra vortex is necessary to counteract the two vortices in respectively the back step and the cavity of the tail.

4.2 Tanker Trailer

Beside rectangular shaped models like the GETS model, also cylindrical shaped vehicles are considered in the research project. Tanker trailer transporting for instance liquids or fluids, use cylindrical shaped trailers. The flow behavior around this type of vehicles is analysed by Saat, [12].
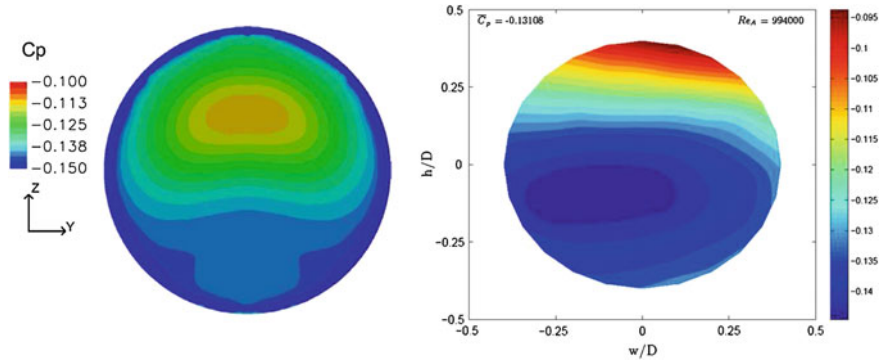
Fig. 17 Rear pressure distribution of a tanker trailer: (l) CFD and (r) wind tunnel analysis

The numerical and experimental pressure distributions at the base of the tank are compared in Fig. 17. As can be seen the general pressure distribution is similar for both analysis tools. The general pressure distribution can be described by relatively low suction at the top of the tank and high suction on the lower. Nevertheless, the difference is that in the numerical C_P-plot the rear stagnation point is located lower on the base, when compared to the measured pressure coefficients. This indicates that in the wind tunnel the lower vortex of the wake is larger in size.

4.3 Combi-Vehicle

Another type of vehicle that has been analysed is the combi-vehilce constisting of a rigid truck together with a drawbar trailer, Buijs [2]. The pressure distribution of the rear surface of the rigid truck and the front surface of the trailer will be compared.

The pressure distributions, see Fig. 18a, b, on the gap surfaces show good resemblances between the wind tunnel measurements and the numerical simulations. The high and lower pressure regions, for both the rigid truck rear (vertical orientation) and trailer front (V-shape orientation) are comparible between the wind tunnel experiments and the numerical simulations. This suggests that the gap flow, for a combi-vehicle is well predicted by numerical analysis, which is not the case for the rear surface of the trailer.

4.4 Rear Shape Modification

For the GETS model a rear shape modification study is executed by Lauwers [11] to analyse different aft concepts and its influence on the drag coefficient. The drag coefficients of the corresponding aft modifications for both CFD and wind tunnel analysis are shown in Fig. 19. The similarity in the trends is clearly notable, when a drag reduction is found with CFD analysis, this is also measured in the wind tunnel.
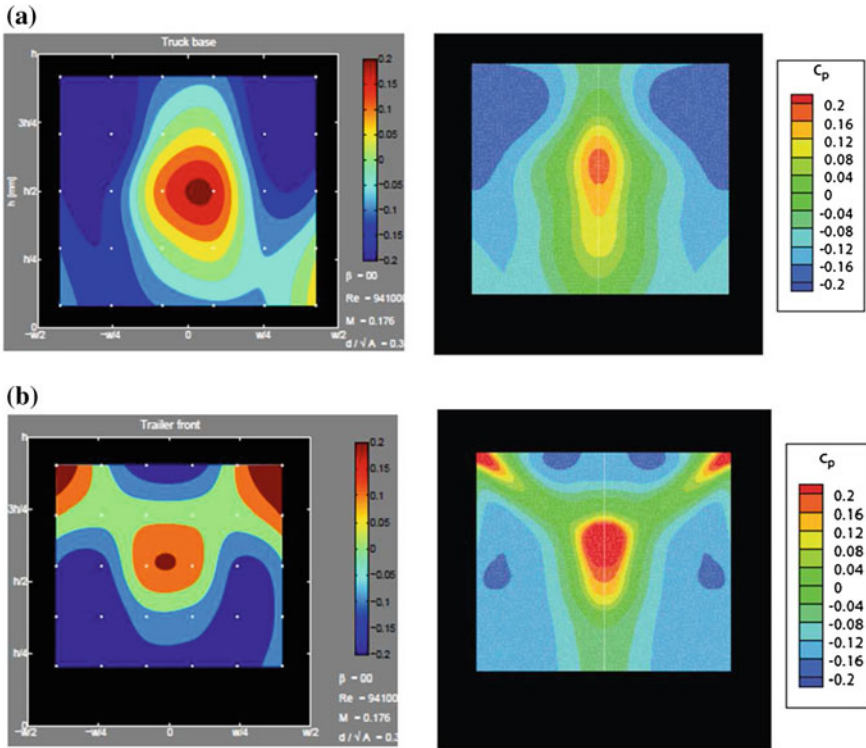
Fig. 18 Pressure distribution truck base (*upper*) and trailer front (*lower*) **a** Pressure distribution rigid truck base (*left*) wind tunnel experiment and (*right*) numerical simulation. **b** Pressure distribution trailer front (left) wind tunnel experiment and (*right*) numerical simulation
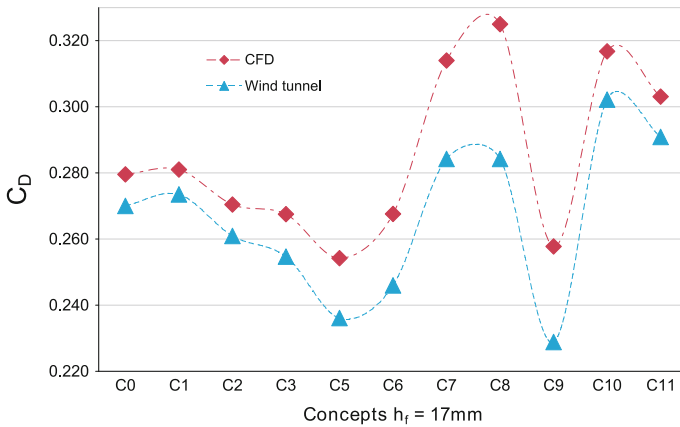

Fig. 19 Comparison of CFD and wind tunnel results for the rear body modifications

The relative improvements of a new concept found by CFD and experimental analysis are very similar. Especially changes in drag coefficients for concept C1, C2, C3, C10 and C11 (all upper aft edge modifications) are almost the same during both methods of analysis. For concepts C5, C6 and C9 (all with the tapered and angled aft surfaces) the CFD analysis predicts a more modest improvement compared to the wind tunnel experiment. The CFD analysis is more pessimistic about concepts C7 and C8 which have both rounded rear side edges and high adverse pressure gradients.

5 Conluding Remarks

A comparison of different flow characteristics of the GETS model is made with the aid of numerical simulations, based on Reynolds Averaged Navier-Stoke equations and wind tunnel experiments.

The absolute numerical obtained values of the drag, lift and mean base pressure coefficient are not exactly in line with the measured coefficients in the wind tunnel. This is mainly due to the numerical modeling and the fact that the underbody flow is not good predicted with the aid of CFD. The drag and side force coefficients of the simulations and measurements agree well for the zero yaw angle case, but the trend agreement decreases for increasing yaw angle. The design example of the aft modifications illustrated that the trend of the different concepts are in good agreement. Only when rear surface modifications imply rear high pressure gradients the numerical simulation overpredict the forces and pressures.

The boundary layer properties, like displacement and momentum thickness and the shape factor, are predicted well with CFD when compared with the scaled analytical equations and wind tunnel experiments. Full-scale and thus high Reynolds number simulations have difficulties to match the theorethical model. Numerical diffusion results in relative thicker boundary layers.

The wake structure obtained from the PIV measurements and the CFD analysis is different in many ways, stating that path lines and flow structures of highly turbulent and separated flow simulated with RANS is insufficient. RANS equations forces the flow in the wake to be steady, while they are highly unstable. This differs from averaging the velocities from an unsteady flow obtained during the PIV experiments. The design example with the standard boat tail illustrated that the resemblance between CFD and wind tunnel experiments is in general positive. The extra vortex at the rear edge of the stepped boat tail is not captured with the numerical simulations. Indicating that detailed flow structures are insufficient simulated with the aid of RANS CFD.

The rear pressure distribution obtained with numerical simulatinos is completely off compared with experimental results. The wind tunnel measurements showed a more lateral pressure distribution while the numerical analysis indicated a central orientated distribution. Applying different turbulence modeling gave no better results. Only LES improved the resemblance with the wind tunnel experiments. The design example with the cylindrical body showed a nicer similarity. Also the pres-

sure distribution in a gap indicated remarquely good similarity between the numerical simulations the wind tunnel experiments.

One has to act carefully when flow patterns and pressure distributions, obtained with RANS simulations of bluff bodies, are considered to design low drag vehicles. The drag and mean pressure coefficients are in good agreement with wind tunnel experiments. If steady numerical simulations are used in the preliminary design phase, only descions based on the relative force and mean pressure coefficients, and not on pressure distributions and flow patterns, should be made before the actual design in the wind tunnel.

References

1. Browand, F., McCallen, R., Ross, J.: Aerodynamics of Heavy Duty Vehicles II: Trucks Busses and Trains. Springer, Berlin (2008)
2. Buijs, L.J.: Numerical and Experimental Analysis on Aerodynamic Solutions for Drag Reduction on Truck-Trailer Combinations. Master's Thesis, Delft University of Technology, Faculty of Aerospace Engineering, The Netherlands (2010)
3. Cooper, K.: The Effect of Front-Edge Rounding and Rear-Edge Shaping on the Aerodynamic Drag of Bluff Vehicles in Ground Approximity. SAE Technical Paper 850288 (1985)
4. Cooper, K.: The Wind Tunnel Testing of Heavy Duty Trucks to Reduce Fuel Consumption. SAE Paper 821285 (1982)
5. Cooper, K.: Bluff-body aerodynamics as applied to vehicle. J. Wind Eng. Ind. Aerodyn. **49**, 1–21 (1993)
6. Freight Best Practice: Aerodynamics of Efficient Road Transport. Department of Transport, UK (2003)
7. Gutierrez, W.T., Hassan, B., Croll, R.H., Rutledge, W.H.: Aerodynamics Overview of the Ground Transportation Systems (GTS) Project for Heavy Duty Drag Reduction. SAE Technical Paper 960906 (1996)
8. Henneman, B.: Modeling of Front Edge Flow Separation on Rounded Bluff Body Bodies Commercial CFD Software, Master's Thesis, Delft University of Technology, Faculty of Aerospace Engineering (2005)
9. Krajnović, S., Davidson, L.: Large-Eddy Simulation of the Flow around a Ground Vehicle Body. SAE Paper, 2001–01-0702 (2001)
10. Lanfrit, M.: Best Practice Guidelines for Handling Automotive External Aerodynamics with FLUENT. Version 1.2. http://www.fluentusers.com (2005)
11. Lauwers, K.: Computational and Experimental Analysis of Trailer Shape Modifications for Drag Reductions. Master's Thesis, Delft University of Technology, Faculty of Aerospace Engineering, The Netherlands (2009)
12. Saat, P.J.W.: Aerodynamic Drag Reduction of Semi-Trailer Tanker Trucks by Means of Tank Base Modification. Master's Thesis, Delft University of Technology, Faculty of Aerospace Engineering, The Netherlands (2010)
13. Schrijvers, P.: Optimizing Towards Minimal Drag of the Aerodynamic Package of a Truck. Master's Thesis, Delft University of Technology, Faculty of Mechanical, Maritime and Materials Engineering, The Netherlands (2010)

14. Society of Automotive Engineers. SAE Wind Tunnel Test Procedure for Truck and Buses. SAE J1252 (1981)
15. Storms, B.L.E.A.: An Experimental Study of the GTS Model in the NASA Ames 7-by 10-FT Wind Tunnel. NASA/TM-2001-209621 (2001)
16. van Dijk, T.N.: Analysis of the Relationship between Front Surface Roughness and the Unsteady Wake behaviour of a Bluff Body. Master's Thesis, Delft University of Technology, Faculty of Aerospace Engineering, The Netherlands (2010)
17. van Ginderdeuren, K.: Design of Guiding Vanes for Bluff Bodies with the aid of Computational Fluid Dynamics. Master's Thesis, Delft University of Technology, Faculty of Aerospace Engineering, The Netherlands (2010)
18. van Leeuwen, P.: Computational Analysis of Base Drag Reduction Using Active Flow Control. Master's Thesis, Delft University of Technology, Faculty of Aerospace Engineering, The Netherlands (2009)
19. van Raemdonck, G.M.R., van Tooren, M.J.L., Boermans, L.: Aerodynamics and Trucks. Platform for Aerodynamic Road Transport, Faculty of Aerospace Engineering—TU Delft, The Netherlands (2009)
20. van Raemdonck, G.M.R., van Tooren, M.J.L.: Time-averaged phenomenological investigation of a wake behind a bluff bofy. In: Bluff Body Aerodynamics and Application VI Conference, Milan, Italy (2008)
21. Vonk, A.F.M.: Stepped Boat Tails on Trucks. Master's Thesis, Delft University of Technology, Faculty of Aerospace Engineering, The Netherlands (2010)